Vibration of a Cantilever Beam with Extended Tip Mass and Axial Load Subject to Piezoelectric Control

MK Moutlana[a], S Adali[b]

Received 29 January 2014, in revised form 21 May 2015 and accepted 8 October 2015

The effect of piezoelectric control on the frequencies of a cantilever beam with an extended tip mass and axial load is studied. Rotatory inertia of the tip mass as well as the stiffness of piezo layers are taken into account and an analytical solution of the problem is obtained by eigenfunction expansions. Displacement feedback control is implemented by bonding ceramic piezoelectric layers on the top and bottom surfaces of the beam. It is noted that the strains caused by the activated piezoelectric layers manifest themselves as moments at the boundary conditions at the free end. Numerical results indicate that the fundamental frequency of the cantilever beam is effectively modified by piezoelectric control. For a beam with extended tip mass and axial load there is a significant reduction in the fundamental frequency. The reduction in the fundamental frequency is limited under certain end conditions. When the tip mass and axial load are large, the changes in frequency becomes insignificant. The results are useful for the design of vibrating cantilever beams with tip mass and under constant axial load.

Additional keywords: Piezoelectric actuator, vibrations, natural frequencies, extended tip mass, axial load

1 Introduction

Vibrations of cantilever beams with tip mass have been studied in a number of papers[1-5] with a view towards assessing the influence of the tip mass on frequencies. One area of application of this mechanical element is atomic force microscopy (AFM), the sensor of which is attached to the tip of a cantilever. The reduction in the fundamental frequency increases the frequency gap between the 1st and 2nd natural frequencies, which allows for a wider range of frequency during operation. The vibrations of AFM cantilevers have been studied extensively in publications[6-11]. In the present study, the vibration characteristics of a cantilever beam with an extended tip mass and subject to an axial load is studied when a displacement feedback control is applied using piezoelectric actuator layers bonded to the top and bottom surfaces. The specific piezo ceramic material is lead zirconium titanate (PZT) and due to the high modulus of elasticity of PZT, the stiffness of the actuators are taken into consideration in the problem formulation. The applicable boundary conditions taking the rotary inertia of the tip mass into account are observed to be time-dependent. The governing differential equation of motion is solved by eigenfunction expansion and the fundamental frequency is computed by solving the characteristic equation numerically. It is observed that piezo control modifies the frequencies of the beam and the extent of the frequency change depends on the magnitude of the tip mass, the length of the moment arm as well as on the axial load being compressive or tensile. Previous studies on the control of beams carrying a tip mass include Fung *et al.*[12] with the control force applied by an electromagnetic actuator and Pratiher[13] where control by electronic damping was investigated. More recently piezo control of cantilever beams with tip mass were studied by Moutlana[14-15].

Vibration control of mechanical elements by piezoelectric actuators, in particular, by piezo actuators made of PZT, is quite common due to the simple procedures involved in its application and the ability of PZT to provide sufficient actuating force[16-20]. A common configuration is a combination of a host beam with piezoelectric layers bonded to the beam surfaces[21-22]. In the publications[16-22], several control algorithms have been formulated to exercise piezo control with the displacement feedback control used by Yang *et al.*[23]. Various approaches to the piezo control of beams can be found in references[24-26]. A survey of vibration control using piezoelectric materials is given by Vasques and Dias Rodrigues[27].

2 Beam with Piezoelectric Layers

The beam under consideration has piezoelectric actuator layers bonded to the top and bottom surfaces as shown in figure 1. The cross-sectional area of the beam is given by $A=bH$, the moment of inertia by $I_c=\frac{1}{12}bH^3$ where $H=h_b+2h_p$ is the total thickness, h_b the beam thickness and h_p the thicknesses of the top and bottom piezoelectric layers. The subscripts b and p refer to the beam and piezo properties, respectively.

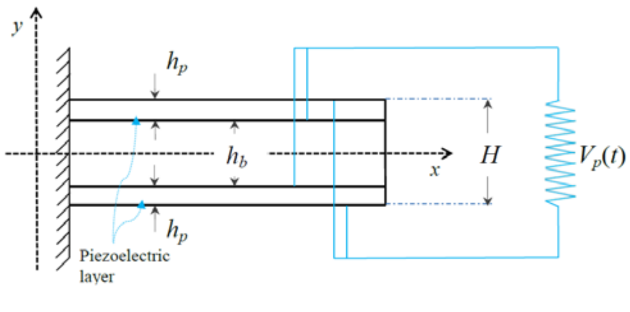

Figure 1: Geometry of the beam with surface bonded piezoelectric actuators

In figure 2, let $w(x,t)$ denote the transverse displacement of the beam. The equation of motion of a freely vibrating beam is derived by Smith[28] and can be expressed as,

$$E_cI_c\frac{\partial^4 w}{\partial x^4}+N\frac{\partial^2 w}{\partial x^2}+\frac{\partial^2 M_p(x,t)}{\partial x^2}+\rho A\frac{\partial^2 w}{\partial t^2}=0 \tag{1}$$

---

a. Department of Mechanical Engineering, Durban University of Technology, Durban

b. Discipline of Mechanical Engineering, University of KwaZulu-Natal, Durban adali@ukzn.ac.za

where $\rho = (h_b\rho_b + 2h_p\rho_p)/H$ is the average density, $M_p(x,t)$ is the moment generated by the piezoelectric actuators, and N is the applied axial load taken positive in compression and negative in tension as shown in figure 2.

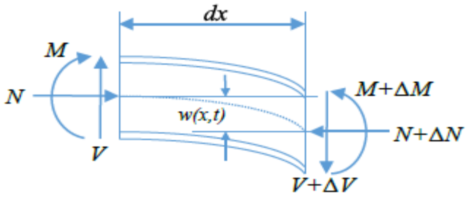

Figure 2: Infinitesimal section of beam in bending with moments and forces

The expression for the combined Young's modulus E_c is given by

$$E_c = \frac{E_p[H^3 - h_b^3] + E_b h_b^3}{H^3} \tag{2}$$

For a piezoelectric layer, strain is given by

$$\varepsilon_{xx}^p = d_{31}E_3 = d_{31}\frac{V_p}{h_p} \tag{3}$$

where d_{31} is the piezoelectricity constant, E_3 is the electric field in the transverse direction and V_p is the applied voltage. The stress-strain relation in each layer of the beam can be expressed as:

(beam layer): $\sigma_{xx} = E_b\varepsilon_{xx}$ (4a)

(piezo layers): $\sigma_{xx} = E_p(\varepsilon_{xx} - \varepsilon_{xx}^p)$ (4b)

where E_b and E_p are Young's moduli of the beam and the piezo layers, respectively. The total moment contributed by the beam and the piezo layers is given by

$$M_z(x,t) = \kappa\int_{A_B} E_c y^2\, dy - M_p(x,t) \tag{5}$$

where $\kappa = 1/r_c$ with r_c denoting the radius of curvature. The combined piezo moment as a function of the tip displacement feedback can be written as:

$$M_p(L,t) = C_0 w(L,t) \tag{6}$$

where

$$C_0 = G\left(\frac{2E_p h_p h_0 + E_b h_b h_0}{2E_p h_p + E_b h_b}\right) \tag{7}$$

where $G=bd_{31}E_p(g_{d1}-g_{d2})$, g_{d1} and g_{d2} are the gain factors for upper and lower piezoelectric layers and $h_0=h_p+h_b$.

3 Method of Solution

Solution of the governing equation (1) is obtained by eigenfunction expansion of the displacement function as

$$w(x,t) = \sum_{n=1}^{\infty} X_n(x)T_n(t) \tag{8}$$

Inserting equation (8) into equation (1) and after rearrangement, we obtain:

$$X_n''''(x) + \beta^2 X_n''(x) - a_n^4 X_n(x) = 0 \tag{9}$$

$$\ddot{T}_n(t) + \omega_n^2 T_n(t) = 0 \tag{10}$$

where $m=\rho A$ and $\rho A = (h_b\rho_b + 2h_p\rho_p)b$, ω_n is the natural frequency for the n^{th} mode of vibration. The axial load parameter β^2 is defined as

$$\beta^2 = \frac{N}{E_c I_c} \tag{11}$$

where $N=kP_{cr}$, $k<1$ is the axial load ratio, and P_{cr} is the critical buckling load. A negative k indicates a tensile load and a positive k indicates a compressive load with the buckling load given by $P_{cr} = (\pi^2 E_c I_c)/4L^2$ for a fixed-free column. The frequency parameter a_n is defined as

$$a_n^4 = \frac{m\omega_n^2}{E_c I_c} \text{ and } a_n = \frac{R_n}{L} \tag{12}$$

where R_n is the n^{th} dimensionless root of the characteristic equation. The general solutions of equations (9) and (10) are given by

$$X_n(x) = A_n \sin p_{2n}x + B_n \cos p_{2n}x + C_n \sinh p_{1n}x + D_n \cosh p_{1n}x \tag{13}$$

$$T_n(x) = E_n \sin \omega_n t + F_n \cos \omega_n t \tag{14}$$

where, p_{1n} and p_{2n} are given by

$$p_{1,2n} = \sqrt{\frac{\mp\beta^2 + \sqrt{\beta^4 + 4a_n^4}}{2}} \tag{15}$$

The constants A_n, B_n, C_n and D_n are determined from the boundary conditions, and E_n and F_n from the initial conditions. The boundary conditions at the clamped end are:

$$w(0,t) = 0; \frac{\partial w(0,t)}{\partial x} = 0 \tag{16}$$

At the free end, the moment and shear boundary conditions are expressed in equation (17) and (18), respectively.

For a beam with extended tip mass (M_T) the centre of gravity of the mass is located at $x=L+d$, where d is the distance from the tip of the beam to the centre of gravity as indicated in figure 3. Taking into account the rotary inertia of the tip mass the boundary conditions[28,29] can be expressed as,

$$E_c I_c \frac{\partial^2 w(L,t)}{\partial x^2} + M_T d\frac{\partial^2 w(L,t)}{\partial t^2} + (J_T + M_T d^2)\frac{\partial^3 w(L,t)}{\partial x \partial t^2} - C_A w(L,t) = 0 \tag{17}$$

$$E_c I_c \frac{\partial^3 w(L,t)}{\partial x^3} + M_T\frac{\partial^2 w(L,t)}{\partial t^2} + M_T d\frac{\partial^3 w(L,t)}{\partial x \partial t^2} - N\frac{\partial w(L,t)}{\partial x} = 0 \tag{18}$$

Where $J_T=M_T(L+d)^2$ is the rotational moment of inertia of the tip mass and

$$C_A = \frac{C_0}{2E_c I_c} \tag{19}$$

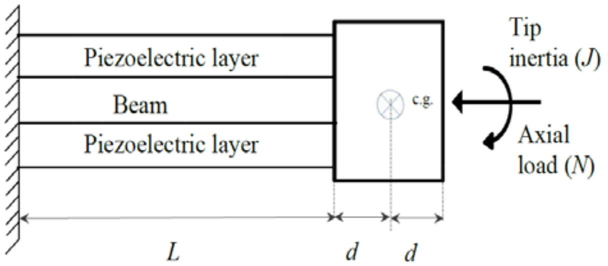

Figure 3: Cantilever beam with an extended tip mass

It is noted that

$$w(L,t) = \sum_{n=1}^{\infty} X_n(L)T_n(t) \tag{20}$$

Substituting equation (20) into equation (17), the following expression is derived:

$$X_n''(L) - d\eta a_n^4 X_n(L) - L^2 \eta a_n^4 X_n(L) - d^2 \eta a_n^4 X_n'(L) - C_A X_n(L) = 0 \qquad (21)$$

where $\eta = M_T/m$ is the tip mass ratio. Substituting equation (20) into equation (18), the shear boundary condition simplifies to the expression:

$$X_n'''(L) + \beta^2 X_n'(L) + d\eta a_n^4 X_n'(L) + \eta a_n^4 X_n(L) = 0 \qquad (22)$$

The solution (13) can be expressed as

$$X_n(x) = C_n\left(\sinh p_{1n}x - \frac{p_{1n}}{p_{2n}}\sin p_{2n}x\right) + B_n(\cos p_{2n}x - \cosh p_{1n}x) \qquad (23)$$

Substituting (23) into the boundary conditions (21) and (22) gives the system of equations

$$\begin{bmatrix} A_{1n} & A_{2n} \\ A_{3n} & A_{4n} \end{bmatrix}\begin{bmatrix} B_n \\ C_n \end{bmatrix} = \begin{bmatrix} 0 \\ 0 \end{bmatrix} \qquad (24)$$

where the expression for A_{in}, i=1,…,4 are given in the appendix. The characteristic equation can be obtained from the determinant of equations (24) as

$$A_{1n}A_{4n} - A_{2n}A_{3n} = 0 \qquad (25)$$

The characteristic equation (25) can be solved numerically for the roots. When the tip mass is zero (η=0) and piezo thicknesses are zero, equation (25) reduces to the frequency equation given in Bokaian[30-31].

4 Control Strategy

The control strategy in this investigation is active displacement feedback control. The tip displacement can be measured using a laser displacement sensor, as indicated in figure 4a.

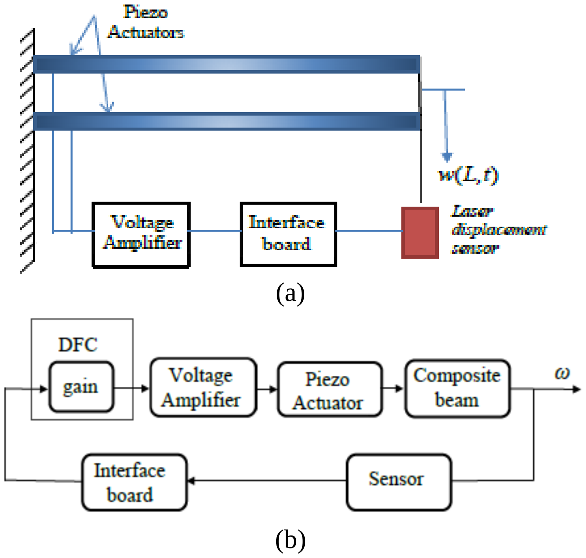

Figure 4: (a) Schematic of control system. (b) Block diagram of feedback control.

The displacement sensor measures the tip displacement and the electromechanical equation of motion is solved using this information. This type of control strategy can be classified under classic control[32].

In equation (17), we note that the tip displacement appears in the moment boundary condition. The measured displacement in combination with the induced potential will have an effect on the boundary conditions and by extension, on the natural frequencies. The natural frequencies can be decreased or increased by varying the voltage potential. Figure 4b shows the block diagram for the feedback loop, where the tip displacement and the gain are coupled to vary the output in terms of vibration frequencies.

5 Numerical results

The dimensions of the beam are chosen the same as the ones used by Bokaian[30-31] to verify the results. Thus the length of the beam is L=0.126 m and the width is b=12.7 mm[30-31]. However the numerical results are given using dimensionless (R_n) values. The properties of the beam and the piezo actuators are shown in table 1.

Table 1: Material and geometric properties of the piezoelectric beam.

	Aluminium beam	Piezo material
Young's Modulus	E_b = 76 GPa	E_p = 59 GPa
Density	ρ_b = 2840 kg/m^3	ρ_p = 1800 kg/m^3
Thickness	h_b = 10 mm	h_p = 1 mm
Piezo Constant (d_{31})	--	260×10^{-12} m/V

Using the characteristic equation (eq. 25) and substituting $a=R/L$ gives us the dimensionless roots R of the characteristic equation. From equation (11) it is noted that these roots are directly associated with the natural frequencies ω. Figures 5 to 8 show the contour plots of the natural frequencies expressed as the dimensionless roots R with respect to axial load ratio and tip mass ratio with varying input voltage. Tables 2 to 5 show the roots R of the characteristic equation (eq. 25).

In figure 5, the lowest natural frequency occurs for a mass load ratio $\eta = 10$ and axial load ratio $k = 0.8$ (compressive), whilst the largest frequency occurs at $\eta = 0$ and k = -2 (tensile).

Table 2 First frequency of a beam with a tip mass and rotary inertia (d = 0) at V = 0 V.

Axial load ratio k	η = 0	η = 0.1	η = 1	η = 5	η = 10
0.8	1.27	1.01	0.63	0.43	0.36
0.4	1.66	1.33	0.83	0.56	0.47
0.2	1.78	1.43	0.88	0.60	0.50
0	1.88	1.51	0.93	0.63	0.53
-0.4	2.03	1.64	1.01	0.67	0.53
-1	2.19	1.78	1.09	0.73	0.62
-2	2.40	1.96	1.18	0.79	0.67

The corresponding results for an active piezo V = 1000 V are given in figure 6. Tables 2 to 5 show a decrease in the natural frequency as the tip mass load ratio increases, and an increase in natural frequency as the axial load ratio transitions from compressive (positive) to tensile (negative) load. When a voltage V = 1000 V is applied along the piezo electric layer we note a general decrease in the natural frequencies as demonstrated in table 3.

From tables 2 and 3 there is a decrease of approximately 48% in frequency for varying tip mass ratios at k = 0.8 and approximately 1.25% for axial load ratio k = -2. It is noted from the data in tables 2 and 3 that the piezo electric actuators lose their effectiveness as the axial load increases in tension.

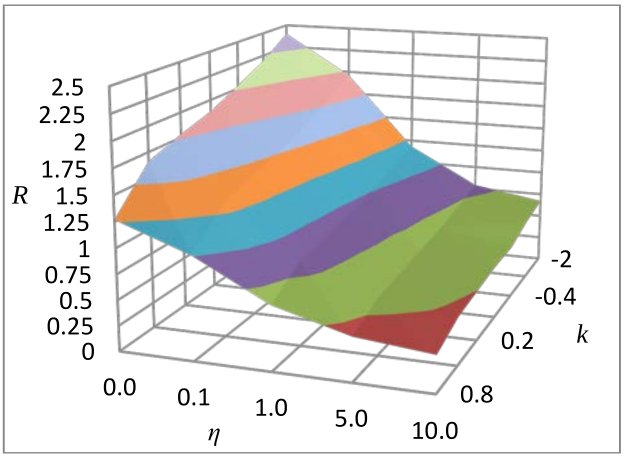

Figure 5: Fundamental frequency vs axial load and tip mass for d = 0 and V = 0 V.

Table 3: First frequency of a beam with a tip mass and rotary inertia (d = 0) at V = 1000 V.

Axial load ratio k	$\eta = 0$	$\eta = 0.1$	$\eta = 1$	$\eta = 5$	$\eta = 10$
0.8	0.66	0.52	0.33	0.22	0.19
0.4	1.53	1.21	0.75	0.51	0.33
0.2	1.68	1.33	0.83	0.56	0.47
0	1.79	1.43	0.88	0.60	0.50
-0.4	1.97	1.58	0.97	0.65	0.55
-1	2.15	1.74	1.06	0.71	0.6
-2	2.37	1.92	1.16	0.78	0.66

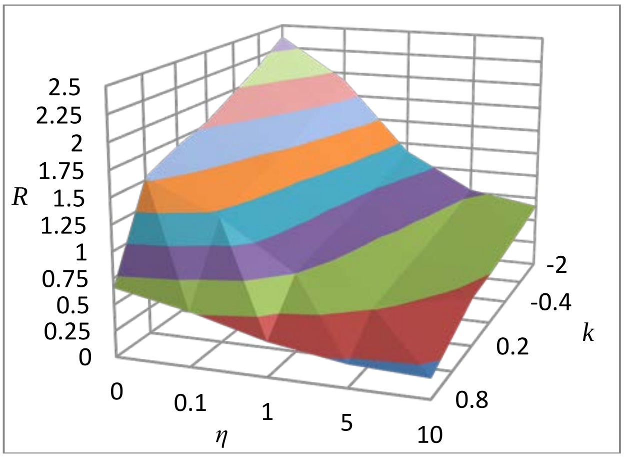

Figure 6: Fundamental frequency vs axial load and tip mass for d = 0 and V = 1000 V.

The results for a cantilever with an extended tip mass, where the centre of gravity of the mass is located at a distance $d = L$ from the tip of the cantilever are given in table 4 and figure 7 which show the contour plots of the frequencies with respect to axial load ratio and the tip mass ratio with zero input voltage. The lowest frequency occurs when $\eta = 10$ and $k = 0.8$, and the largest frequency at $\eta = 0$ and $k = -2$.

The corresponding results for $V = 1000$ V are given in table 5 and figure 8, and a comparison of the lowest frequencies for $V = 0$ V (figure 7) and $V = 1000$ V (figure8) indicates a 49% decrease in the frequencies when $V = 1000$ V. However, this difference is only 1% for varying mass load ratio and the axial load ratio is $k = -2$.

Table 4: First frequency of a beam with a tip mass and rotary inertia ($d = L/1$) at V = 0 V.

Axial load ratio k	$\eta = 0$	$\eta = 0.1$	$\eta = 1$	$\eta = 5$	$\eta = 10$
0.8	1.25	0.85	0.50	0.34	0.28
0.4	1.66	1.12	0.66	0.44	0.37
0.2	1.78	1.20	0.70	0.47	0.40
0	1.88	1.26	0.74	0.50	0.42
-0.4	2.03	1.37	0.80	0.53	0.45
-1	2.19	1.48	0.86	0.58	0.49
-2	2.40	1.62	0.94	0.63	0.53

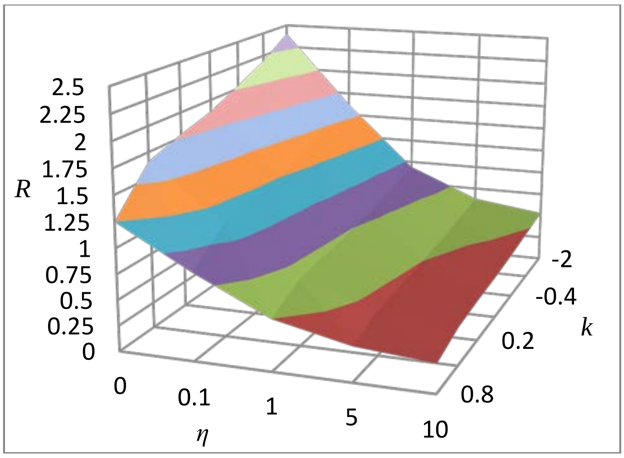

Figure 7: Fundamental frequency vs axial load and tip mass for $d = L$ and V = 0 V.

In tables 2 and 4 the natural frequencies are identical for $\eta = 0$ as expected, and this also applies to tables 3 and 5. If the tip mass is zero, the magnitude of the distance d from the tip of the beam is immaterial. When $\eta > 0$ the distance d from the tip of the beam must be taken into account and the natural frequencies for $d = 0$ are smaller than the natural frequencies for $d = L$ and as a result of the rotary inertia of the tip mass.

Table 5: First frequency of a beam with a tip mass and rotary inertia ($d = L/1$) at V = 1000 V.

Axial load ratio k	$\eta = 0$	$\eta = 0.1$	$\eta = 1$	$\eta = 5$	$\eta = 10$
0.8	0.66	0.44	0.26	0.18	0.15
0.4	1.53	1.02	0.6	0.4	0.34
0.2	1.68	1.12	0.66	0.44	0.37
0	1.79	1.20	0.7	0.47	0.40
-0.4	1.97	1.32	0.77	0.51	0.43
-1	2.15	1.44	0.84	0.56	0.47
-2	2.37	1.59	0.92	0.62	0.52

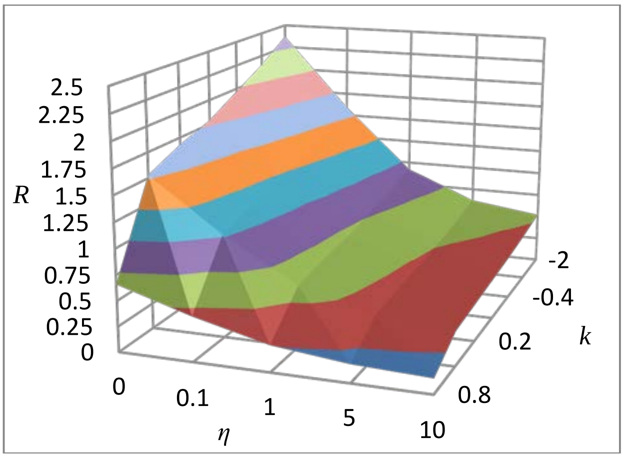

Figure 8: Fundamental frequency vs axial load and tip mass for $d = L$ and $V = 1000$ V.

6 Conclusions

The effects of piezoelectric layers acting as actuators on the frequencies of a cantilever beam with a tip mass and subject to an axial load are studied. The piezoelectric composite beam is made of two actuator layers of equal thickness bonded to the top and bottom surfaces of the host beam. The control is specified as displacement feedback control with the deflection of the free end of the beam providing the feedback. The effect of the vibration control is investigated in the presence of rotary inertias of the tip mass. Also included in the computations are compressive or tensile external axial loads which can accentuate or nullify the piezo control. The mechanical effect of the activated piezoelectric layers is observed to be a boundary moment at the free end of the beam, which results in modifying the natural frequencies of the beam.

The solution for the actively controlled cantilever beam is obtained analytically by expanding the deflection in terms of its eigenfunctions and solving the resulting characteristic equation numerically. The results are given in the form of three dimensional plots in terms of the fundamental frequencies, magnitude of the tip mass and the axial load. In the numerical examples, the maximum applied voltage is specified as 1000V per 1mm thickness of the piezo layers. It is observed that the piezo actuators are more effective in modifying the fundamental frequency when the axial load is compressive. It is noted that the actuation becomes less effective as the tip mass increases. Another observation is the piezo layer become less effective as the moment arm of the tip mass becomes larger.

In this case a moment arm is introduced and the analysis also takes rotary inertia into consideration. The effect of rotary inertia is to lower the frequencies. A concentrated mass yields higher natural frequencies compared to those of an extended mass with inertia. Both the concentrated and extended mass have the effect of lowering of the natural frequencies.

The first mode is the fundamental mode and the most important in the analysis of the system. The vibrations on the piezo electric beam are affected by piezo actuation most significantly in the fundamental mode. The second modes are affected minimally and the reductions in the natural frequencies in the higher modes are considered negligible.

Acknowledgement

The research of the second author was supported by research grants from the University of KwaZulu-Natal (UKZN) and from National Research Foundation (NRF) of South Africa. The author gratefully acknowledges the support provided by UKZN and NRF.

References

1. *Abramovich H and Hamburger O*, Vibration of a cantilever Timoshenko beam with a tip mass, *Journal of Sound and Vibration*, 1991, 148(1), 162-170.
2. Farghaly SH, Bending vibrations of an axially loaded cantilever beam with an elastically mounted end mass of finite length, *Journal of Sound and Vibration*, 1992, 156(2), 373-380.
3. *Auciello NM*, Transverse vibrations of a linearly tapered cantilever beam with tip mass of rotary inertia and eccentricity, *Journal of Sound and Vibration*, 1996, 194(1), 25-34.
4. *Hassanpour PA, Cleghorn WL, Mills JK and Esmailzadeh E*, Exact solution of the oscillatory behavior under axial force of a beam with a concentrated mass within its interval, *Journal of Vibration and Control*, 2007, 13(12), 1723–1739.
5. *Li XF, Tang AY and Xi LY*, Vibration of a Rayleigh cantilever beam with axial force and tip mass, *Journal of Constructional Steel Research*, 2003, 80, 15-22.
6. *Wu T-S, Chang W-J and Hsu J-C*, Effect of tip length and normal and lateral contact stiffness on the flexural vibration responses of atomic force microscope cantilevers, *Microelectronic Engineering*, 2004, 71(1), 15-20.
7. *Mahdavi MH, Farshidianfar A, Tahani M, Mahdavi S and Dalir H*, A more comprehensive modeling of atomic force microscope cantilever, *Ultramicroscopy*, 2008, 109(1), 54-60.
8. *Hsu J-C, Lee H-L and Chang W-J*, Flexural vibration frequency of atomic force microscope cantilevers using the Timoshenko beam model, *Nanotechnology* 2007, 18(28), 285503.
9. *Lee H-L and Chang W-J*, Coupled lateral bending–torsional vibration sensitivity of atomic force microscope cantilever, *Ultramicroscopy*, 2008, 108(8), 707-711.
10. *Mokhtari-Nezhad F, Saidi AR and Ziaei-Rad S*, Influence of the tip mass and position on the AFM cantilever dynamics: Coupling between bending, torsion and flexural modes, *Ultramicroscopy*, 2009, 109(9), 1193-1202.
11. *Abbasi M and Mohammadi AK*, A new model for investigating the flexural vibration of an atomic force microscope cantilever, *Ultramicroscopy*, 2010, 110(11), 1374-1379.
12. *Fung R-F, Liu Y-T and Wang CC*, Dynamic model of an electromagnetic actuator for vibration control of a cantilever beam with a tip mass, *Journal of Sound and Vibration*, 2005, 288(4), 957-980.

13. *Pratiher B*, Vibration control of a transversely excited cantilever beam with tip mass, *Archive of Applied Mechanics*, 2012, 82(1), 31-42.
14. *Moutlana MK*, Effect of piezoelectric control on a cantilever beam with extended tip mass and axial load. *Proceedings of the 1st International Conference on Composite and Biocomposites and Nanocomposites* (ICCBN-1), 2 – 4 December 2013, Durban, South Africa, 555-575
15. *Moutlana MK*, Use of piezo actuators to maximize the fundamental frequency and the frequency gaps *Proceedings of the 9th South African Conference on Computational and Applied Mechanics*, 14 – 16 January 2014, Somerset West.
16. *Wang Q and Quek ST*, Flexural vibration analysis of sandwich beam coupled with piezoelectric actuator, *Smart Materials and Structures*, 2000, 9(1), 103–109.
17. *Yim W and Singh SN*, Adaptive output feedback force control of cantilever beam using piezoelectric actuator, *Journal of Vibration and Control*, 2003, 9(5), 567-581.
18. *Xu L*, *Ling S-F*, *Lu B*, *Li H and Hu H*, Sensing capability of a PZT-driven cantilever actuator, *Sensors and Actuators A: Physical*, 2006, 127(1), 1-8.
19. *Gurses K*, *Buckham BJ and Park EJ*, Vibration control of a single-link flexible manipulator using an array of fiber optic curvature sensors and PZT actuators, *Mechatronics*, 2009, 19(2), 167-177.
20. *Yuvaraja M and Senthilkumar M*, Comparative study on vibration characteristics of a flexible GFRP composite beam using SMA and PZT actuators, *Procedia Engineering*, 2013, 64, 571-581.
21. *Gaundenzi P*, *Carbonaro R and Benzi*, *E*, Control of beam vibrations by means of piezoelectric devices: Theory and experiments, *Composite Structures*, 2000, 50(4), 373-379.
22. *Brissaud M*, *Ledren S*, *Gonnard P*, Modeling of a cantilever non-symmetric piezoelectric bimorph, *Journal of Micromechanics and Microengineering*, 2003, 13(6), 832-844.
23. *Yang Y*, *Ju C and Soh CK*, Analytical and semi-analytical solutions for vibration control of a cantilevered column using a piezoelectric actuator, *Smart Materials and Structures*, 2003, 12(2), 193–203.
24. *Kayacık O*, *Bruch JC Jr.*, *Sloss JM*, *Adali S and Sadek IS*, Integral equation approach for piezo patch vibration control of beams with various types of damping. *Computers and Structures*, 2008, 86(3), 357–366.
25. *Spier C*, *Bruch JC Jr.*, *Sloss JM*, *Adali S and Sadek IS*, Placement of multiple piezo patch sensors and actuators for a cantilever beam to maximize frequencies and frequency gaps, *Journal of Vibration and Control*, 2009, 15, 643-670.
26. *Spier C*, *Bruch JC Jr.*, *Sloss JM*, *Adali S and Sadek IS*, Analytical and finite element solutions for active displacement feedback control using PZT patches. *Journal of Vibration and Control*, 2010, 16(3), 323-342.
27. *Vasques CMA and Dias Rodrigues J*, Active vibration control of smart piezoelectric beams: Comparison of classical and optimal feedback control strategies, *Computers and Structures*, 2006, 84(22), 1402–1414.
28. *Smith RC*, Smart Materials Systems: Model Development, SIAM, Philadelphia, 2005.
29. *Magrab EB*, Vibrations of elastic systems: With applications to MEMS and NEMS, New York, Springer, 2012.
30. *Bokaian A*, Natural frequencies of beams under compressive axial loads, *Journal of Sound and Vibration*, 1988, 126(1), 49-65.
31. *Bokaian A*, Natural frequencies of beams under tensile axial loads, *Journal of Sound and Vibration*, 1990, 142(3), 481-498.
32. *Amezquita-Sanchez JP*, *Dominguez-Gonzalez A*, *Sedghati R*, *de Jesus Romero-Troncoso R*, *and Osornio-Rios RA*, Vibration control on smart civil structures: A review, *Mechanics of Advanced Materials and Structures*, 2014, 21(1), 23–38.

Appendix

The values of A_{in}, $i = 1,\ldots,4$ appearing in equation (23) are given below:

$$A_{1n} = P_{1n}\cosh(p_1L) - P_{2n}\cos p_2L + R_{1n}\left(\frac{p_1}{p_2}\sin p_2L + \sinh(p_1L)\right)$$

$$A_{2n} = \frac{p_1}{p_2}P_{2n}\sin p_2L - P_{1n}\sinh p_1L + R_{1n}(\cos p_2L - \cosh(p_1L))$$

$$A_{3n} = R_{2n}p_2\sin p_2L - R_{3n}\sinh(p_1L) + a_n^4\eta(\cos p_2L - \cosh(p_1L))$$

$$A_{4n} = \frac{p_1}{p_2}R_{2n}p_2\cos p_2L + R_{4n}\cosh(p_1L) + a_n^4\eta\left(\frac{p_1}{p_2}\sin p_2L - \sinh(p_1L)\right)$$

where

$$P_1 = a_n^4 d\eta + C_A - p_1^2,$$
$$P_2 = a_n^4 d\eta + C_A + p_2^2,$$
$$R_1 = a_n^4 p_1\eta(d^2 + L^2),$$
$$R_2 = a_n^4 d\eta + p_2^2 - \beta^2,$$
$$R_3 = a_n^4 d\eta p_1 + p_1^2 - \beta^2 p_2,$$
$$R_4 = -a_n^4 d\eta p_1 + p_1^3 + \beta^2 p_2.$$